



Tectonics

RESEARCH ARTICLE

10.1002/2014TC003584

Key Points:

- Mapping in Taiwan gives information on fault reactivation at shelf-slope break
- Identify an important, northeast striking lateral structure
- *P* wave model points to the presence of a basement culmination

Correspondence to:

J. Alvarez-Marron,
jalvarez@ictja.csic.es

Citation:

Alvarez-Marron, J., D. Brown, G. Camanni, Y.-M. Wu, and H. Kuo-Chen (2014), Structural complexities in a foreland thrust belt inherited from the shelf-slope transition: Insights from the Alishan area of Taiwan, *Tectonics*, 33, 1322–1339, doi:10.1002/2014TC003584.

Received 11 MAR 2014

Accepted 23 MAY 2014

Accepted article online 5 JUN 2014

Published online 10 JUL 2014

Structural complexities in a foreland thrust belt inherited from the shelf-slope transition: Insights from the Alishan area of Taiwan

Joaquina Alvarez-Marron¹, Dennis Brown¹, Giovanni Camanni¹, Yih-Min Wu², and Hao Kuo-Chen³

¹Institute of Earth Sciences Jaume Almera, ICTJA-CSIC, Barcelona, Spain, ²Department of Geosciences, National Taiwan University, Taipei, Taiwan, ³Institute of Geophysics, National Central University, Jhongli, Taiwan

Abstract The Alishan area of Taiwan spans the transition from the platform with full thickness of the Eurasian continental margin in the north to the thinning crust of its slope in the south. This part of the foreland thrust and fold belt includes important along-strike changes in structure, stratigraphy, and seismic velocities. In this paper we present the results of new geological mapping from which we build geological cross sections both across and along the regional structural trend. Fault contour, stratigraphic cutoff, and branch line maps provide 3-D consistency between the cross sections. Minimum shortening is estimated to be ~15 km with displacement overall to the northwest. A *P* wave velocity model helps constrain the structure at depth by providing insight into the possible rock units that are present there. *P* wave velocities of ≥ 5.2 km/s point toward the presence of basement rocks in the shallow subsurface throughout much of the southeastern part of the area, forming a basement culmination. The changes in strike of thrusts and fold axial traces, the changing elevation of thrusts and stratigraphic contacts, and the growing importance of Middle Miocene sediments that take place from north to south are interpreted to be associated with a roughly northeast striking lateral structure coincident with the northern flank of this basement culmination. These transverse structures appear to be associated with the inversion of Eocene- and Miocene-age extensional faults along what was the shelf-slope transition in the Early Oligocene, uplifting the margin sediments and their higher *P* wave velocity basement during Pliocene-Pleistocene thrusting.

1. Introduction

The oblique collision that is taking place in Taiwan between the southeastern part of the continental margin of Eurasia and the leading edge of the intraoceanic Philippine Sea Plate means that the entire profile of the margin, from the full thickness of the crust (platform) in the north to the thinning crust of the slope toward the ocean-continent transition just offshore southern Taiwan, is now involved in the deformation within the foreland thrust and fold belt [e.g., Teng, 1990; Huang *et al.*, 1997; Teng and Lin, 2004; Hsu *et al.*, 2004; Lin *et al.*, 2003, 2008; Eakin *et al.*, 2014] (Figure 1). This makes Taiwan an ideal laboratory in which to study the importance that the preexisting structural architecture and the different morphological parts of a continental margin have on the early evolution of a foreland thrust and fold belt. The extensional tectonic history of the southeastern margin of Eurasia began with rifting in the Early Eocene and culminated with the development of oceanic crust in the South China Sea by Late Eocene to Early Oligocene times [e.g., Sibuet and Hsu, 1997, 2004; Lin *et al.*, 2003; Li *et al.*, 2007]. At this time the shelf-slope break (or necking zone of Mohn *et al.* [2012]) was located just north of its current position [cf. Teng, 1987; Lin *et al.*, 2003] (see inset for Figure 1). Rifting resulted in a number of deep, roughly northeast trending basins that were filled with Eocene-age clastic sediments and then unconformably overlain by Oligocene-age sediments [Teng, 1992; Lin *et al.*, 2003, 2008; Teng and Lin, 2004]. Extension on the outer part of the margin (slope), although minor, was also widespread during the Middle to Late Miocene [Lin *et al.*, 2003; Ding *et al.*, 2008], resulting in the development of a number of extensional basins and changes in the associated Miocene stratigraphy. A number of models have been proposed for how the convergent history between the Eurasian and Philippine Sea plates progressed from intraoceanic subduction in the Miocene to today's arc-continent collision [e.g., Suppe, 1984; Teng, 1987; Lee and Lawver, 1994; Hall, 1996, 2001; Sibuet and Hsu, 1997, 2004; Yu *et al.*, 1997; Malavielle *et al.*, 2002; Li *et al.*, 2007]. All agree that the Philippine Sea Plate in the vicinity of Taiwan is moving northwestward relative to Eurasia (Figure 1) and that since about the Middle Miocene the subduction zone has advanced westward, causing the leading edge of the Philippine Sea Plate to obliquely override the slope of the continental margin in that direction (see, for example, the GPS data of

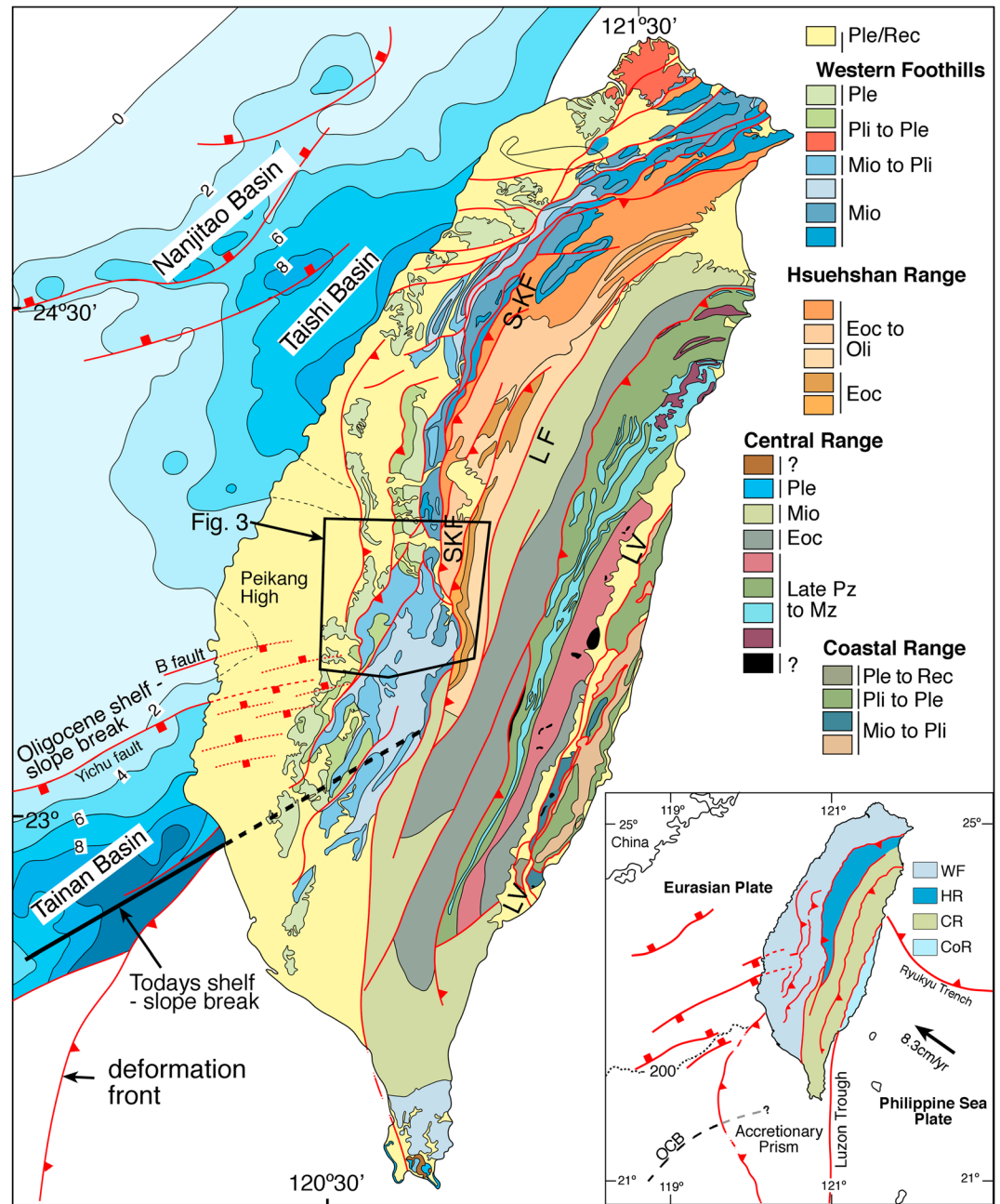


Figure 1. Geological map of Taiwan [after *Chen et al.*, 2000]. Basin locations and structure in the Taiwan Strait is from *Teng and Lin* [2004]. Contours in the offshore basins denote the depth to the top of the Mesozoic basement. The locations of the B and Yichu faults are shown, as are the current shelf-slope break and its estimated location along the southern flank of the Peikang high at the beginning of the Oligocene. The location of Figure 3 is also shown. SKF = Shuilikeng fault, LF = Lishan fault, LV = Longitudinal Valley. The inset shows the tectonostratigraphic units and the tectonic setting discussed in the text (WF = Western Foothills, HR = Hsuehshan Range, CR = Central Range, CoR = Coastal Range). The convergence vector of 8.3 cm/yr between the Philippine Sea Plate and the southeastern part of the Eurasian Plate is also given. OCB = ocean-continent boundary, and the -200 isobath marks the current shelf-slope break. East of the Luzon Trough is the Luzon arc.

Yu et al. [1997] and *Ching et al.* [2011]). In this scenario, the ocean-continent transition, the Early Oligocene and today's shelf-slope break, and the major extensional basins on the slope of the continental margin in the southwest of Taiwan (all oriented approximately N60°E) are nearly perpendicular to the convergence vector but highly oblique to the westward advance of the overriding upper plate [*Lin et al.*, 2003; *Hsu et al.*, 2004; *Yeh and Hsu*, 2004; *Yu et al.*, 1997; *Yu*, 2004; *Li et al.*, 2007; *Ching et al.*, 2011] (Figure 1).

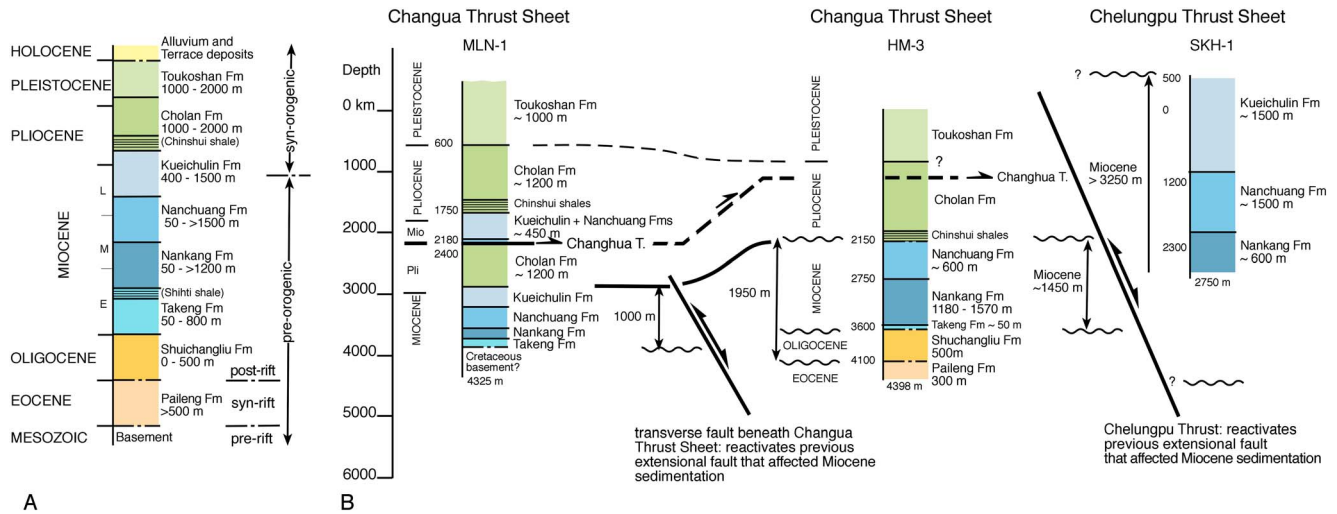


Figure 2. (a) Simplified stratigraphic column showing the formation names discussed in the text. (b) Stratigraphic columns of boreholes MLN-1, HM-3, and SKH-1 (taken from *Chiu* [1975] and *Yang et al.* [2007]) with an interpretation of the relationships between them. The interpreted location of the Changhua thrust in HM-3 is shown.

The Early Oligocene change from platform to slope in the southeast Eurasian margin took place across the Alishan area (Figure 1). This makes the Alishan area of particular interest for the study of how inherited structural and sedimentological features of the continental margin are influencing the development of this part of the foreland thrust and fold belt. With this aim, and also to further the understanding of this important area in the geology of Taiwan, we present the results of new geological mapping and geological cross sections that we integrate with available borehole data, and a *P* wave (*V_p*) velocity model. The 3-D interpretation obtained for the structure of the Alishan area provides insights on the role that inherited continental margin features play during the development of thrust systems. For the sake of clarity, throughout the paper, a distinction is made between the Alishan area (shown by the box in Figure 1) and the topographic feature of the Alishan Ranges.

2. Geological Background

2.1. Tectonostratigraphic Zones of Taiwan

The Taiwan orogen can be divided into four roughly N-S oriented tectonostratigraphic zones (Figure 1). These zones are separated by major faults and comprise parts of the continental margin and the colliding volcanic arc [Teng, 1992; Huang et al., 1997; Lin et al., 2003; Sibuet and Hsu, 1997, 2004]. From west to east these zones are the Western Foothills, the Hsuehshan Range, the Central Range, and the Coastal Range. The Western Foothills, Hsuehshan Range, and Central Range are formed as the result of shortening and uplift of the continental margin of Eurasia [Suppe, 1980; Yue et al., 2005; Mouthereau et al., 2001]. The Coastal Range is composed of volcanic rocks and sedimentary basins of the Luzon arc, which is accreting obliquely and end-on to the Eurasian margin along the Longitudinal Valley fault [Yu and Kuo, 2001; Chen et al., 2007; Shyu et al., 2008]. In this paper we focus on the Alishan area, part of the Western Foothills in what is geographically known as central Taiwan (Figure 1).

2.2. Stratigraphy

The stratigraphy of the Alishan area determined from outcrop and borehole data comprises Mesozoic to recent sediments (Figure 2a). The Mesozoic rocks are predominantly Cretaceous (with minor Jurassic) prerift clastic sediments of the Eurasian margin basement of southeast China [Chiu, 1975; Ho, 1988; Jahn et al., 1992]. Above this basement there are Eocene synrift clastic sediments that are unconformably overlain by Early to Late Oligocene clastics [Chiu, 1975; Ho, 1988; Teng, 1992; Shaw, 1996; Lin et al., 2003; Teng and Lin, 2004]. The Early Oligocene unconformity is interpreted to represent the rift-to-drift transition (or breakup unconformity) in the margin and its subsequent thermal subsidence during the opening of the South China Sea [Teng, 1992; Huang et al., 1997, 2001; Lin et al., 2003; Teng and Lin, 2004]. Oligocene rocks are not present everywhere [Chiu, 1975; Shaw, 1996; Lin et al., 2003]. Where present they are conformably overlain by Neogene clastics, and where they are not present, the Neogene may unconformably overlie either the Eocene or the Mesozoic [Lin et al., 2003, 2008]. The

Miocene largely comprises preorogenic shallow water sediments deposited along a delta front within several systems of Miocene-age rift basins [Ho, 1988; Lin *et al.*, 2003]. The Late Miocene through Holocene rocks make up the synorogenic sediments to the Taiwan orogen. Thickness changes on the order of several hundreds to greater than 1000 m are common in all of the preorogenic sequences [e.g., Chiu, 1975; Ho, 1988; Shaw, 1996], both across thrusts and within a single thrust sheet [Yang *et al.*, 2007; Tensi *et al.*, 2006; Rodriguez-Roa and Wiltschko, 2010]. For example, the Miocene sequences increase in thickness from ~1000 m in borehole MLN-1 to ~1500 m in borehole HM-3, and more than 2750 m in borehole SKH-1 (Figure 2b). Our mapping suggests that these changes are in part due to structural repetitions within individual formations (see below).

The nomenclature used for the various stratigraphic units throughout the Western Foothills is variable (for an overview of this problem, see Yang *et al.* [2007], Tensi *et al.* [2006], and Rodriguez-Roa and Wiltschko [2010]). Therefore, in this work we have adopted the nomenclature shown in Figure 2a. It maintains continuity with that used in our previous mapping to the north of Alishan [Brown *et al.*, 2012; Camanni *et al.*, 2014], which is based on the stratigraphic sequence presented in the Central Geological Survey 1:50,000 scale map 32 (Puli) [Huang *et al.*, 2000]. The only difference here is that we have changed the name Shihmen Formation to Nankang Formation, which is the more generally used name in this area. The ages are consistent with correlations done by Shea *et al.* [2003] and Tensi *et al.* [2006].

Cretaceous rocks do not outcrop in the study area, but have been reported from several boreholes in western Taiwan [Chiu, 1975; Jahn *et al.*, 1992]. Their thickness is unknown. About 300 m of Eocene rocks have been intersected in borehole HM-3 (Figure 2b), although their base was not reached [Chiu, 1975; Shaw, 1996]. In our cross-section interpretations, the thickness of the Eocene ranges from 500 to > 1000 m and it is called the Paileng Formation. Oligocene rocks do not crop out in the study area, but they have also been intersected in borehole HM-3 (Figure 2b) where they are up to ~500 m thick [Chiu, 1975]. We therefore use this as the maximum thickness for the Oligocene, letting it thin and disappear eastward where the Miocene directly overlies the Eocene. We call the Oligocene rocks the Shuichangliu Formation.

The Miocene rocks are divided into four formations (Figure 2a) that, from bottom to top, are the Early Miocene Takeng Formation, the Early to Middle Miocene Nankang Formation (part of it corresponds with the Shihmen Formation), the Middle to Late Miocene Nanchuang Formation, and the Late Miocene to Early Pliocene Kueichulin Formation. The Takeng Formation only outcrops in the NE part of the map area, in the core of the Takeng anticline, where it is approximately 500 to 800 m thick, although the base is not seen. The Nankang Formation outcrops along much of the eastern part of our map area, where it comprises predominantly highly folded and faulted Shihti shale (the basal part on Nankang), hampering a determination of the stratigraphic thickness. Borehole SHK-1 intersected about 600 m of Nankang Formation without reaching its base (Figure 2b). The Nanchuang Formation outcrops throughout the map area, although several kilometers to the north it is absent within the Miocene sequence. In many areas it is intensely folded and faulted making it difficult to estimate its thickness. In the eastern part of our map area, along the southern part of the Chenyulan River (Figure 3), the Nanchuang Formation is approximately 800 m thick, whereas in the west, along the Cingshui River, we have mapped a little over 1000 m of it. Borehole SHK-1 (Figure 3) intersects ~1500 m of Nanchuang but does not mention folding. The latest Miocene to Early Pliocene Kueichulin Formation has very significant changes in thickness in the map area, ranging from about 2000 m thick in the hanging wall of the Chelungpu thrust to ~500 m thick in the Lukushan syncline (Figure 3). The SHK-1 borehole intersected ~1500 m of Kueichulin Formation (Figure 2b).

There is some uncertainty as to whether or not the Kueichulin Formation is the first synorogenic sedimentary unit to appear in the foreland basin of the Taiwan mountain belt. Yu and Chou [2001]; Lin and Watts [2002], and Lin *et al.* [2003] argue on the basis of geometric relationships observed between the Nanchuang and the Kueichulin Formations in reflection seismic data that there is an angular unconformity between the two that marks the onset of synorogenic sedimentary deposition in the foreland basin. Teng [1987]; Covey [1986], and Hong [1997] suggest, however, that the first appearance of slate clasts derived from the rising Taiwan mountain belt to the east is in the Pliocene Chinshui shale, and that these are the first synorogenic sediments. We place the onset of synorogenic sedimentation within the Kueichulin Formation (Figure 2a).

The Chinshui shale comprises a several hundred meter thick unit at the base of the Pliocene to Pleistocene Cholan Formation. The Cholan Formation comprises up to 2500 m of interbedded mudstone, shale, and sandstone. To the north of the Choshui River (and within the map area), the contact between the Cholan and the

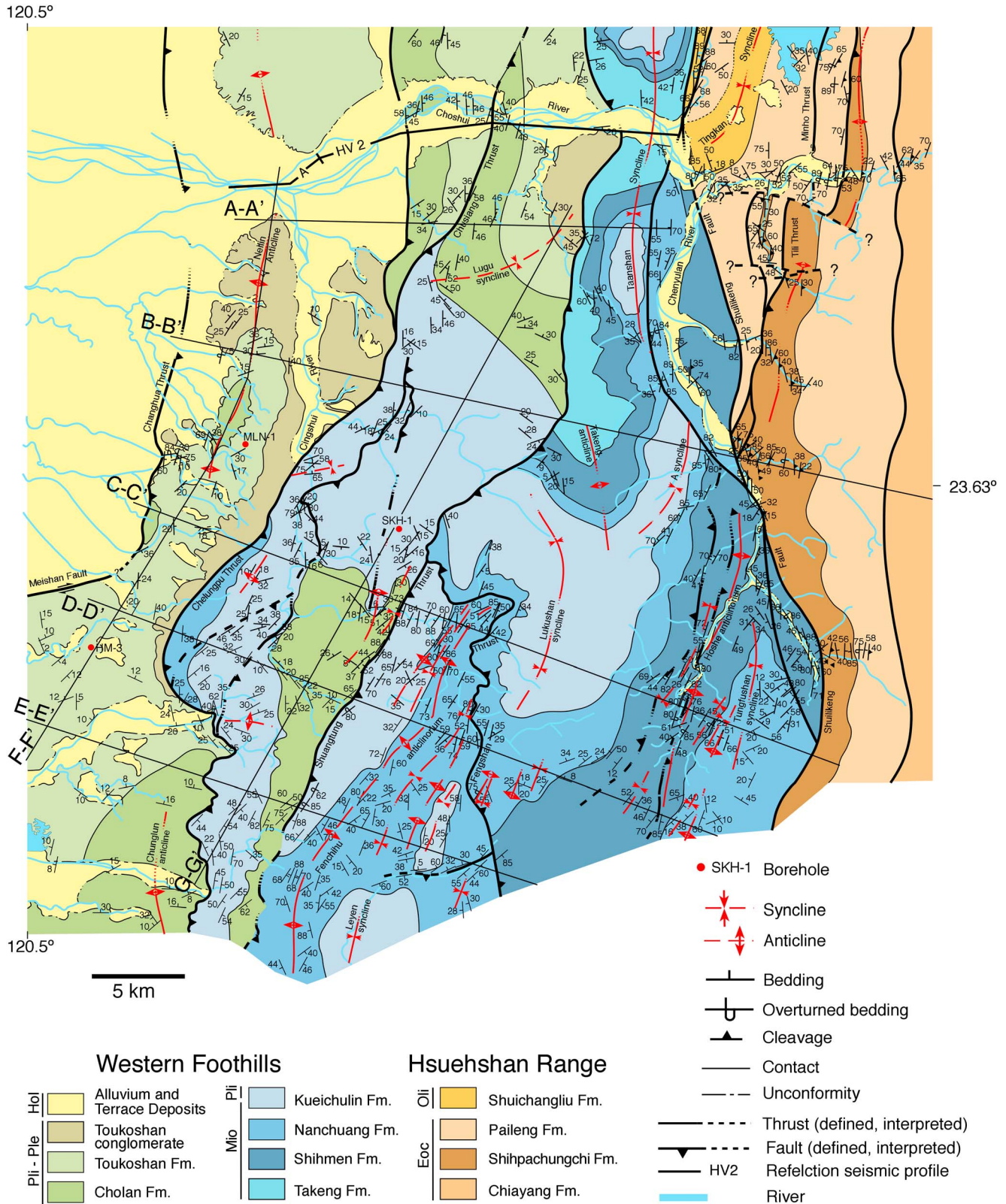


Figure 3. Geological map of the Alishan area. Section A is from *Brown et al.* [2012]. The locations of the geological sections shown in Figures 4 and 5 are shown. Sections A to E also correspond to the locations of the vertical *P* wave velocity sections shown in Figure 8. The names of individual structures discussed in the text are also provided. The locations of reflection seismic lines A and HV 2 from *Wang et al.* [2002] are given.

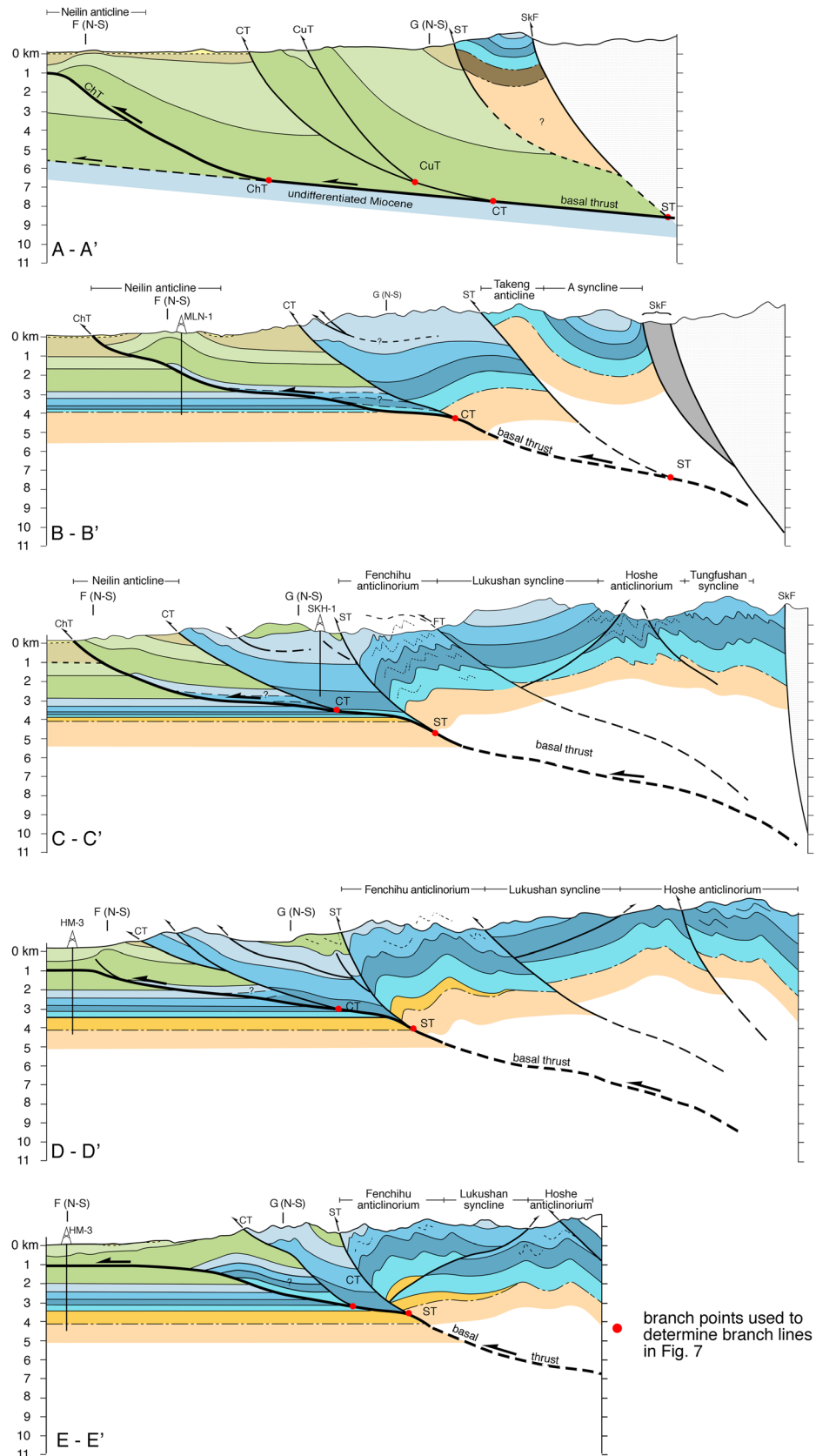


Figure 4

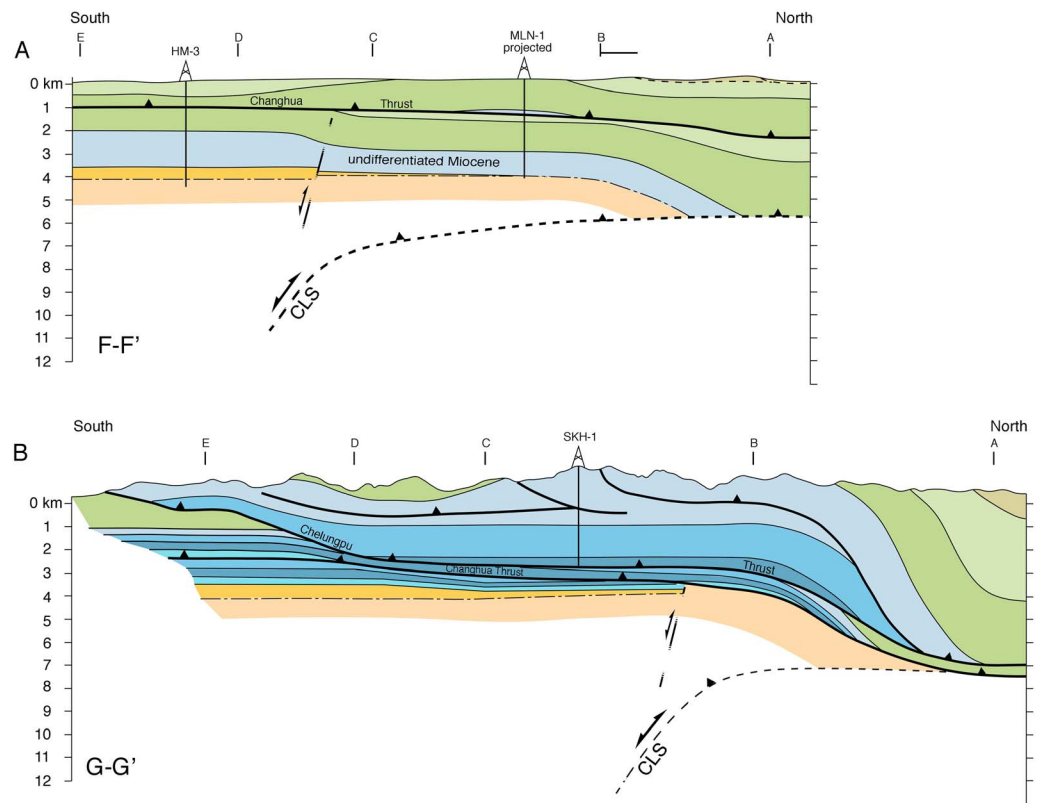


Figure 5. Roughly along strike geological sections F-F' and G-G' (see Figure 3 for location) through (a) the Changhua and (b) the Chelungpu thrust sheets. The projected location of the boreholes is shown. Note the shallowing in elevation of thrust surfaces and stratigraphic contacts toward the south, between sections A and B. A transverse fault beneath the Changhua thrust in F-F' corresponds to that mentioned in Figure 2. CLS = Choshui lateral structure.

Kueichulin formations is not exposed but is thought to be tectonic [e.g., Yue *et al.*, 2005; Yang *et al.*, 2007; Rodriguez-Roa and Wiltschko, 2010], whereas to the south it is a conformable sedimentary contact [e.g., Nagel *et al.*, 2013] (see also section 3 below). The Cholan Formation is conformably overlain by the Pleistocene Toukoshan Formation, a coarsening upward sequence made up of thick-bedded sandstone with shale interbeds that, upward, becomes interfingered with, and eventually completely replaced by conglomerate. The Toukoshan Formation can reach up to 4000 m in thickness. To the south of the Alishan area (and out of our map area), the Toukoshan Formation conglomerate disappears as the Pleistocene in that area was deposited in a marine environment that was typically nearshore to foreshore [Covey, 1984; Chen *et al.*, 2001; Nagel *et al.*, 2013]. The Toukoshan Formation is overlain by Holocene-age gravels that, in places, are several hundred meters thick.

3. Structure of the Alishan Area

3.1. Methodology

A number of authors [e.g., Yang *et al.*, 2006, 2007; Mouthereau and Lacombe, 2006; Rodriguez-Roa and Wiltschko, 2010; Tsai *et al.*, 2012] have investigated the structure of parts of the Alishan area, generally presenting cross sections that are largely based on the 1:100,000 geological map [Chinese Petroleum Company (CPC), 1986], borehole, and reflection seismic data of the Chinese Petroleum Company (CPC). In this study, new geological field mapping was carried out at a 1:50,000 scale over most of the Alishan area; the easternmost part was mapped at 1:25,000 scale [Camanni *et al.*, 2014]. Where available, the 1:50,000 scale

Figure 4. Geological cross sections through the Alishan area. Their locations are shown in Figure 3. The projected locations of the boreholes are shown. The names of individual structures discussed in the text are also provided. The branch points used to construct the maps in Figure 6 are also given. ChT = Changhua thrust, CT = Chelungpu thrust, ST = Shuangtung thrust, FT = Fengshan thrust, and SkF = Shuilikeng fault.

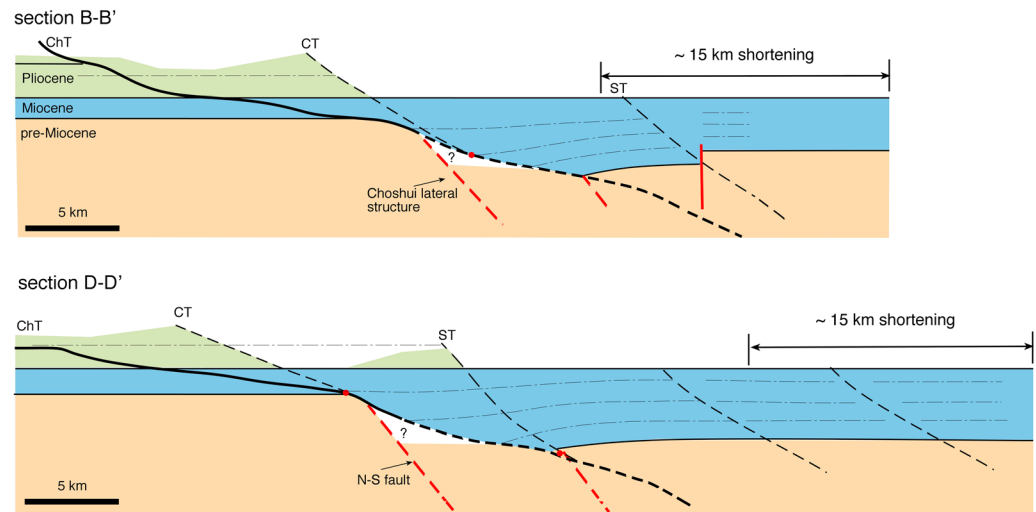


Figure 6. Restored sections B-B' and D-D'. Both sections have been restored using only the Pliocene, Miocene, and pre-Miocene sedimentary packages while conserving the area and line length. In the restoration it is assumed that the top of the Kueichulin is horizontal. Vertical and horizontal scales are the same. The estimated minimum shortening is 15 km. Fault abbreviations are as in Figure 4. See.

geological maps of the Central Geological Survey and the CPC 1:100,000 scale map [CPC, 1986] were used as reference maps. The geological map (Figure 3), structural data, and cross sections presented below are, however, our own. The stratigraphic scheme used in the mapping (Figure 2a) is based on a number of sources [e.g., CPC, 1986; Huang *et al.*, 2000; Chiu, 1975; Ho, 1988] and our own observations. In the description of the structure that follows, the map area is divided into the Changhua, Chelungpu, and Shuangtung thrust sheets forming a linked thrust system. Cross sections have been constructed in several orientations in order to better illustrate the 3-D variation of the structures (Figures 4 and 5). The cross sections were constructed using standard techniques in which the location of faults in the shallow subsurface (~5 km) is determined using the geometric controls provided by the observed outcropping and borehole stratigraphic contacts and the bedding dips [e.g., Dahlstrom, 1969; Hossack, 1979]. Boreholes HM-3, MLN-1, and SKH-1 provide further constraints on the frontal part of some cross sections, in the Changhua and Chelungpu thrust sheets. Two of the sections have been line length and area balanced, and restored (Figure 6). We stress, however, that errors may have been introduced into the cross sections because of the uncertainties in the stratigraphic thicknesses [e.g., Judge and Allmendinger, 2011; Allmendinger and Judge, 2013]. Therefore, fault contour and branch line maps with hanging wall and footwall stratigraphic cutoff lines are used to maintain consistency between all sections (Figure 7). These maps, together with the two restored sections, provide minimum estimates of shortening and displacement directions.

3.2. The Changhua Thrust Sheet

The Changhua thrust sheet is bound to the west by the Changhua thrust and to the east by the Chelungpu thrust. In the southernmost part of the map area the Changhua thrust interacts in some indeterminate way with the Meishan fault (Figure 3). In our interpretation the Meishan fault acts as a lateral tear fault to the Changhua thrust. Some map interpretations [e.g., CPC, 1986; Liu *et al.*, 2004; Mouthereau and Lacombe, 2006; Yang *et al.*, 2007; Rodriguez-Roa and Wiltschko, 2010] extend the Changhua thrust (with a different name) farther southward, but we have not found any evidence for this in our surface mapping. Although we interpret the buried Changhua thrust to be at ~1000 m depth in borehole HM-3 (Figures 2 and 4). In the northern part of the map area it is also buried, but has been imaged by reflection seismic data along the Choshui River (Figure 3) and intersected in borehole MLN-1 (Figure 2) [Wang *et al.*, 2002]. Only two outcrops of the Changhua thrust were found during our mapping; both in the central part of the map area where it places Toukoshan Formation sandstones on top of Holocene gravels. The Neilin anticline, in the hanging wall of the Changhua thrust, plunges between 5° and 25° both northward and southward. It is cored by rocks of the Cholan Formation and locally has a steep to overturned forelimb and a gently dipping backlimb. Northward, it plunges beneath the Holocene gravels along the Choshui River (Figure 3).

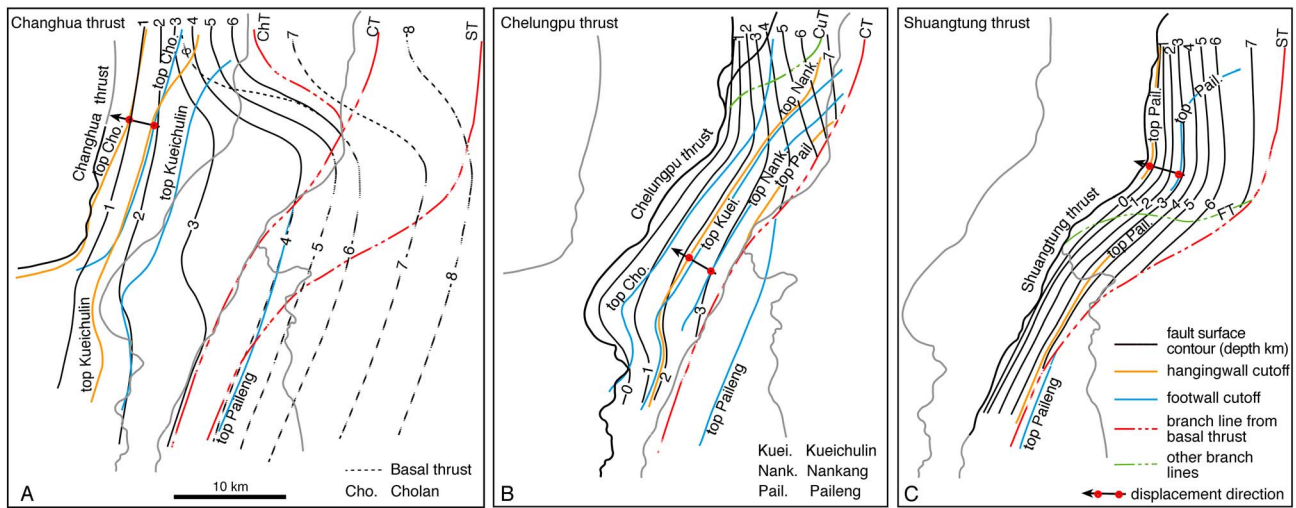


Figure 7. Maps of (a) the contours of the basal thrust surface with the branch lines of the Changhua, Chelungpu, and Shuangtung thrusts. Various hanging wall and footwall stratigraphic cutoffs in the Changhua thrust sheet. The contours for the Changhua thrust are shown as solid lines beginning at the branch line. The displacement direction of the Changhua thrust is shown by the arrow. (b) Contours of the Chelungpu thrust, its branch line from the basal thrust, and various hanging wall and footwall stratigraphic cutoffs. The branch line of the Chusiang thrust is also shown. The displacement direction of the Chelungpu thrust is shown by the arrow. (c) Contours of the Shuangtung thrust and its branch line from the basal thrust. The displacement direction of the Shuangtung thrust is shown by the arrow. The branch line of the Fengshan thrust is also shown. A general displacement direction of about N70°W can be determined from these reconstructions. Thrust abbreviations are the same as those in Figure 4. Numbers represent depth of contour in km.

Southward, the Neilin anticline disappears and immediately below the Chelungpu thrust there is an area with widely dispersed, shallow bedding dips that form the open Chunglun anticline (Figure 3).

We could not find outcrops of the Meishan fault, although there is a topographic expression left from the 1906 7.1 M_L Meishan earthquake. Based on fault plane solutions of recent earthquakes the Meishan fault is interpreted to be a dextral strike slip fault [e.g., Wu *et al.*, 2010], which is in keeping with different map interpretations in the area [CPC, 1986; Liu *et al.*, 2004]. The Meishan fault appears to form part of the eastern extension of the B and Yichu faults (Figure 1) and is interpreted to be so in what follows.

In the cross sections shown in Figure 4, the Changhua thrust is the frontal expression of the basal thrust, extending from the branch points of the Chelungpu thrust to the surface, except in section A-A' where it ramps from the basal thrust. The Changhua thrust has been interpreted to be predominately within the synorogenic sediments (Figures 4 and 5) before ramping gently down into the Miocene formations toward the east and south (except in section A-A'). There is a significant change in depth of the Changhua thrust along strike, from ~7 km deep in the north to about 3 km in the south (compare the branch points of Chelungpu thrust (CT) between sections A-A' and E-E' in Figure 4, as well as section G-G' in Figure 5b), as it climbs progressively up the stratigraphic section in its footwall. The hanging wall and footwall cutoff maps (Figure 7a) of the top Cholan and Kueichulin Formations indicate that the displacement along the Changhua thrust was overall toward the west-northwest. By restoring these cutoffs along the displacement direction the horizontal displacement of the Changhua thrust is estimated to be approximately 5 km in section A-A' and lessening southward to about 2.5 km (Figure 6). Note that in cross sections A-A', D-D', and E-E', the tip line is buried by the synorogenic sediments, as shown in the seismic line farther north [Wang *et al.*, 2002] (Figure 3). Our interpretation of the shallowing of the Changhua thrust southward from the Choshui River is in agreement with other cross sections through the area [e.g., Mouthereau and Lacombe, 2006; Yang *et al.*, 2007; Rodriguez-Roa and Wiltschko, 2010], although our estimations of displacement vary.

3.3. The Chelungpu Thrust Sheet

The Chelungpu thrust sheet is bound to the west by the Chelungpu thrust and to the east by the Shuangtung thrust. It includes the Chusiang thrust to the north and displays important changes southward. North of the Choshui River it carries only rocks of the Cholan and Toukoshan Formations, whereas southward the Chelungpu thrust merges with the Chusiang thrust and cuts down the stratigraphic section to involve the

Kueichulin and Nanchuang Formations (Figure 3). The hanging wall of the Chusiang thrust comprises the northeast plunging Lugu syncline. Immediately southward, the Kueichulin Formation has a number of minor thrusts within it, although it is often not possible to trace these faults for long distances. Nevertheless, they appear to form a thrust system that may significantly thicken the Kueichulin Formation (borehole SHK-1 intersects some 1500 m of Kueichulin Formation in this area). The base of the Cholan Formation in this part of the Chelungpu thrust sheet is at greater than 1400 m above sea level, indicating a large change in elevation of this contact with respect to its depth of ~7 km below sea level along the Choshui River (Figure 5b) [see also, Yue *et al.*, 2005; Yang *et al.*, 2007; Rodriguez-Roa and Wiltschko, 2010; Brown *et al.*, 2012].

In cross section, the Chelungpu thrust is interpreted to be at the base of the Cholan Formation in the north (section A-A'), whereas southward it ramps down section to form a flat near the top of the Nanchuang Formation (Figure 4). This interpretation is in keeping with others in this area [e.g., Yang *et al.*, 2007; Rodriguez-Roa and Wiltschko, 2010], although some authors interpret it to cut steeply down into the Miocene and older rocks along the Choshui River [e.g., Yue *et al.*, 2005; Mouthereau and Lacombe, 2006]. Despite ramping down the stratigraphic section southward, the depth of the Chelungpu thrust and its branch line shallows along strike from ~7 km deep along the Choshui River (section A-A') to ~3 km farther south (sections D-D' and E-E'): a roughly 4 km change in elevation (Figure 5b). Hanging wall and footwall stratigraphic cutoffs indicate that the displacement direction was overall northwestward (Figure 7b). The amount of displacement along the Chelungpu thrust is difficult to determine because of the change in stratigraphic thicknesses that take place across it. Nevertheless, we estimate that the horizontal displacement is ~7 km throughout the Alishan area (Figure 6), which is in keeping with other cross-section interpretations in the area [e.g., Yang *et al.*, 2007; Rodriguez-Roa and Wiltschko, 2010]. Because of the increase in thickness of the Miocene stratigraphy across the Chelungpu thrust (Figure 2b), we interpret it to have reactivated a previous extensional fault (Figure 6).

3.4. The Shaungtung Thrust Sheet

The Shuangtung thrust sheet is bound to the west by the Shuangtung thrust and to the east by the Shuilikeng fault. The thrust sheet widens significantly from less than 5 km along the Choshui River to ~25 km in the central part of the Alishan Ranges (Figure 3). As it does, the Miocene stratigraphic sequence thickens and the Nanchuang Formation becomes an important stratigraphic unit. The Shuangtung thrust sheet comprises two regional-scale fault panels that are separated by the Fengshan thrust. The eastern part of the Shaungtung thrust sheet is dominated by the Hoshe anticlinorium (and the smaller Tungfushan syncline). The Hoshe anticlinorium comprises a system of northwest verging, variably plunging folds that terminate northward against the Shuilikeng fault [Camanni *et al.*, 2014] and can be traced southward for several kilometers before they are lost in an area without access (Figure 3). A number of mostly northwest verging thrusts (there is one significant exception to this) have been mapped, but their along-strike continuity is difficult to constrain. The Hoshe anticlinorium is flanked to the west by the broad, flat-bottomed Lukushan syncline. Access to much of the area occupied by the Lukushan syncline is restricted, and the area is heavily forested, making field and remote sensing observations difficult. The Lukushan syncline is bound to the west by the Fengshan thrust. The thrust panel below the Fengshan thrust is comprised by the Fenchiu anticlinorium, a system of northwest verging, variably plunging folds developed in the Nanchuang and Kueichulin Formations. The Fengshan thrust appears to be a splay off the Shuangtung thrust, but difficulty in accessing the area in the steep topography where the two merge makes the interpretation of how these two faults interact somewhat uncertain.

In cross section, at the surface the Shuangtung thrust is a steep reverse fault, dipping ~80° (this is well-constrained in sections C-C', D-D', and E-E'). The regional-scale structure of the Shaungtung thrust sheet in the Alishan area is that of a dome consisting of two anticlinoria separated by the Lukushan syncline. Pervasive, km-scale folding in the Shuangtung thrust sheet is indicative of significant horizontal shortening. While it is not possible to quantify the shortening because of uncertainties in the stratigraphy, we estimate the horizontal shortening across the Shuangtung thrust to be less than 5 km and the displacement direction is toward the west-northwest (Figures 6 and 7c). Using the stratigraphic template given in Figure 2 there does, however, appear to be an important amount of vertical displacement (see, for example, the elevation of the Takeng Formation in the Takeng anticline). This can be interpreted based on two points. First, in the northern part of the map area the involvement of the Takeng Formation (the base of the Miocene) in the

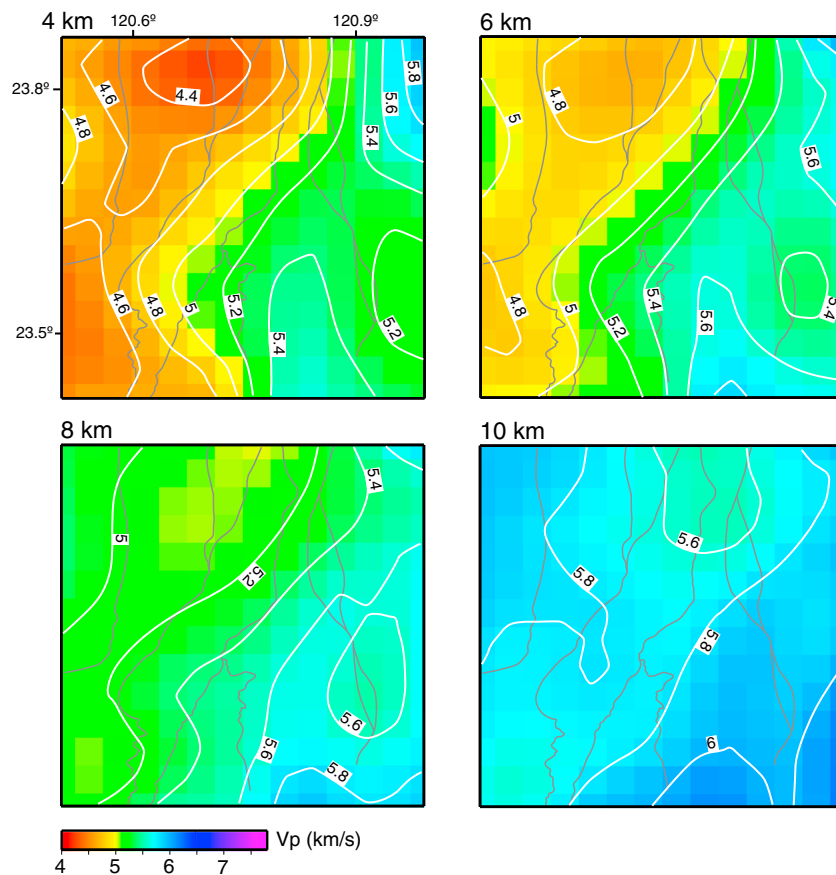


Figure 8. Horizontal cuts at 4, 6, 8, and 10 km depth through the *P* wave velocity model with various isovelocity lines shown.

thrusting indicates that the Shuangtung thrust penetrates to at least this level in the stratigraphy and perhaps deeper. Second, in our interpretation, the branch points of the Shaungtung thrust is interpreted to mark the location in which the basal thrust ramps down eastward into the Eocene synrift and, we think, the basement rocks (Figures 4, 6, and 7) (see section 5). The branch line of the Shuangtung thrust indicates that it changes from southeast to east dipping as it deepens toward the northeast (Figure 7c).

4. Tomography Data

4.1. Methodology

To further constrain the structure at a depth greater than 5 km, especially within and beneath the Shuangtung thrust sheet, we use the *P* wave (*V_p*) velocity model derived from the TAIGER “local” tomography [Kuo-Chen *et al.*, 2012]. The horizontal resolution of the model in the Alishan area is 4 km by 4 km, and the vertical resolution is 2 km. See Kuo-Chen *et al.* [2012] for an overview of the model setup and the data handling. Horizontal slices were cut at various depths through the Alishan area (Figure 8), and vertical sections (Figure 9) were cut along the line of the west-east geological cross sections shown in Figure 4.

4.2. *P* Wave Velocity Model

Within the upper 8 km of the crust in the Alishan area there is a marked change in *V_p* from less than 4.4 km/s in the northwest and west to greater than 5.6 km/s in the southeast (Figure 8). This is outlined by the change in strike of the 4.6 through to 5.4 km/s isovelocity lines from roughly north-south in the north to a northeast-southwest across the Alishan area. This change in strike roughly coincides with similar changes in the strikes of the Chelungpu and Shuangtung thrusts at the surface (shown in gray in Figure 8). The *V_p* model clearly indicates the presence of a shallow velocity high in the southeast part of the area, especially in the area of the Shuangtung thrust sheet. At a depth of 10 km the velocities range between 5.6 and 5.8 km/s, indicating that rocks with similar

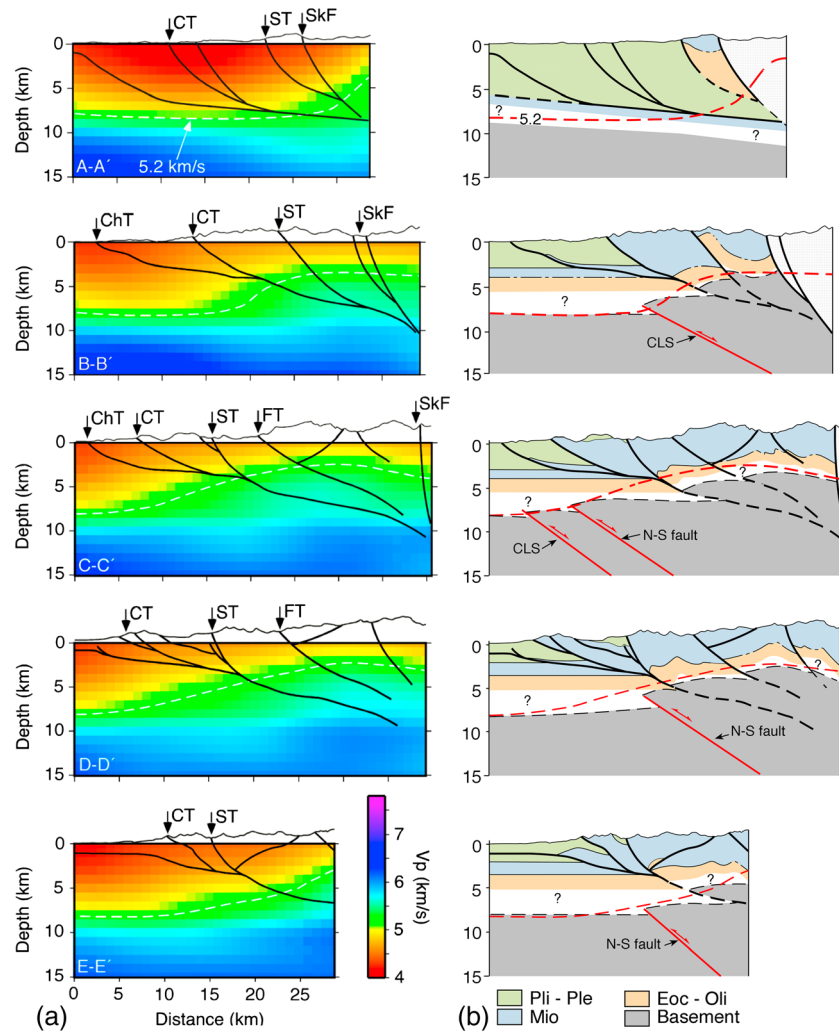


Figure 9. (a) Vertical sections through the P wave velocity model with the fault interpretations taken from Figure 3 plotted on them. The locations are shown in Figure 3. The 5.2 km/s isovelocity line is shown. Thrust abbreviations are the same as those in Figure 4. (b) Simplified geological cross sections from Figure 4 with an interpretation of the basement constrained by the V_p model. Note that we do not interpret the structure east of the Shuilikeng fault (SkF). CLS = Choshui lateral structure. CLS and the N-S fault are shown in Figure 10.

physical properties are widespread at this depth. We interpret these velocities to image the presence of basement rocks everywhere at this depth within the Alishan area (Figure 9) (also see section 5).

In the vertical sections, low velocities (<4.6 km/s) in the west and northwest correspond to the Miocene and younger sediments (Figure 9). The pronounced west to east shallowing of higher velocities starts beneath the Chelungpu thrust sheet and takes on a dome-shape in the area of the Shuangtung thrust sheet. This is particularly well-illustrated by the 5.2 km/s isovelocity line as it shallows from ~ 8 km depth in the west to about 3 km depth in the Shuangtung thrust sheet (Figures 4 and 8). We interpret this feature as a shallowing of the basement rocks as it is uplifted by reverse activation of two deep faults, one striking N-E that we name the Choshui lateral structure (CLS) (see Figure 5), and another striking approximately N-S (Figure 9b) (also see section 5).

5. Discussion

The Alishan area of Taiwan provides new data on the importance of the morphological and structural architecture in the early convergent history of a rifted continental margin. It encompasses the shelf-slope break (or necking zone), which is known to be an area of change in the amount of extension, from low β factors on the platform to increasingly higher β factors on the slope and with, commonly, a corresponding

change in fault style from high angle to listric [e.g., *Manatschal, 2004; Reston, 2009; Reston and Manatschal, 2011; Mohn et al., 2012*]. The structure of the Alishan area presented in this paper shows that the change in basement structure from the platform to the slope, together with changes in the postrift sedimentary carapace all play a significant role early on in the structural history of the thrust belt evolution. In many orogens worldwide, the involvement of the platform or slope in the deformation can be shown to have taken place, but it is not always straightforward from the final rock record exactly how or when this happened [e.g., *Flöttmann and James, 1997; Faulds and Varga, 1998; Smith, 1999; Butler et al., 2006; Zanchi et al., 2006; Yagupsky et al., 2008*]. This makes the Alishan area of considerable importance in placing more precise constraints on the early stages of development of a thrust belt within the complex structural and sedimentological context that is the shelf-slope break of a continental margin.

The new surface geological data and velocity models presented above confirm that there are significant changes that take place in the structure from north to south across the Alishan area. These observations coincide with interpretations by *Rodriguez-Roa and Wiltschko [2010], Yang et al. [2006, 2007], and Mouthereau and Lacombe [2006]*, but adding more data to, for example, the change in strike and detachment level of the fault and fold systems. The location and geometry of the basal thrust to the east of the branch line with the Chelungpu thrust is not well constrained. But interpolating geometries in 3-D of hanging wall and footwall stratigraphic cutoffs and the fault contours (Figures 4–6) from those of the better constrained Changhua and Chelungpu thrusts to the basal thrust provides the model with consistency. One of the important results of our study is that the estimated minimum shortening across the Alishan area is about 15 km. As stated in section 3.1, we realize that there are uncertainties in this estimation, but they are overall in keeping with the shortening calculated by *Rodriguez-Roa and Wiltschko [2010], Mouthereau and Lacombe [2006]* and *Yang et al. [2007]* do not provide shortening for all of Alishan. Another of the important results is that while the Changhua and Chelungpu thrusts cut down the hanging wall stratigraphic section toward the south, they also display a 4 km shallowing in elevation. This change in elevation is perhaps best visualized by comparing the location of the contact between the Cholan and Kueichulin formations in the southern limb of the Lugu syncline, which shows a ~7 km change in elevation from north to south (Figures 3 and 5b). In their cross sections, *Yang et al. [2007]* also interpret (but do not explicitly say) that there is a shallowing of the Changhua and Chelungpu thrusts southward from the Choshui River to the Alishan area, whereas *Rodriguez-Roa and Wiltschko [2010]* do not interpret this to happen. *Mouthereau and Lacombe [2006]* have both thrusts ramping continuously down section. Finally, while we make certain assumptions about the changes in thickness of sediments of all ages, the appearance of the Nanchuang Formation in the Miocene and its increasing importance southward across the Alishan area is obvious and significant. We interpret the changes in strike of the faults and fold axial traces, the change in elevation of the Changhua and Chelungpu thrusts, the change in elevation of stratigraphic contacts, and the growing importance of the Nanchuang Formation, all of which take place from north to south across the Alishan area, to be associated with a roughly northeast striking feature that we call the Choshui lateral structure (Figure 10).

Many of the structural and stratigraphic changes that we outline above have been attributed to the Alishan area being located along the southern flank of the Peikang High [e.g., *Mouthereau et al., 2002; Cheng et al., 2003; Wu et al., 2007; Byrne et al., 2011*], which comprises a number of approximately east-northeast trending extensional faults in the footwall to the exposed thrust system. Many of these are buried beneath synorogenic sediments but have been either imaged in reflection seismic data or sampled in boreholes [*Yang et al., 1991; Chen and Yang, 1996; Lin et al., 2003*]. The Meishan fault (Figure 3) is a notable exception to this. In map view, a number of these faults are often grouped and represented by two major faults called the “B” and Yichu faults [e.g., *Chen and Yang, 1996; Lin et al., 2003*] (Figure 1). Most known faults along the southern flank of the Peikang High are thought to be Miocene in age [*Lin et al., 2003, 2008; Ding et al., 2008*], although Eocene-age extensional faults have also been interpreted to occur in this area [*Lin et al., 2003, 2008; Li et al., 2007; Tang and Zheng, 2010*]. The Peikang High itself is interpreted as an Eocene-age feature with the Taishi and Hsuehshan basins to the north and east, respectively [e.g., *Lin et al., 2003*]. To the south of it are the shelf-slope break (Alishan), the slope, and finally the ocean-continent transition of the Eurasian margin. We therefore interpret some of the faults affecting the basement along the southern flank of the Peikang High to be Eocene in age, and that this area formed the shelf-slope transition (or necking zone) of the Eurasian margin at the time of continental break up in the Early Oligocene. The present day shelf-slope break is farther south (Figure 3) due to the progradation of the Miocene to recent sediments onto the slope [*Ho, 1988; Yu and Lin, 1991*]. Other features, such

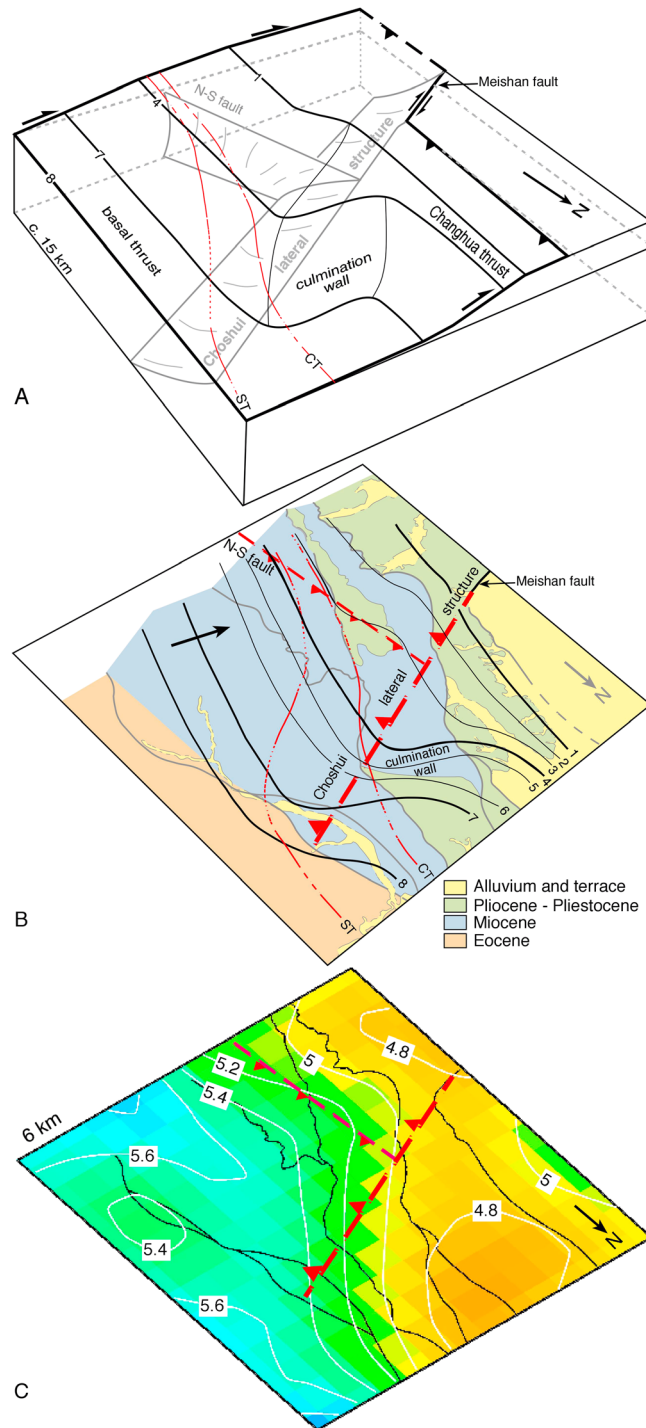


Figure 10. (a) Schematic diagram showing the interpreted 3-D hanging wall and footwall structure to the basal thrust system across the Alishan area. Numbers represent depth of contours in km. The terminology used in the text is explained. Note that the footwall structure is shown in gray, whereas the basal thrust surface is shown by contours in black. The Meishan fault, which is part of the B and Yichu fault system, is interpreted to be related to the Choshui lateral structure. Fault abbreviations are as in Figure 4. (b) Simplified geological map rotated into the same orientation as Figure 10a. The basal thrust contours, the Shuangtung and Chelungpu cut-off lines, the Choshui lateral structure, and the lateral culmination wall are shown. Black arrow indicates the general transport direction of thrusts and is oblique to both the N-S fault and the CLS. Fault abbreviations are as in Figure 4. (c) Horizontal cut at 6 km depth through the *P* wave velocity model with the location of the N-S fault and the CLS. It is rotated into a similar orientation as Figures 10a and 10b.

as the changes in thickness of the Miocene sediments, and the increasing importance of the Nanchuang Formation southward can be attributed to the widespread Middle to Late Miocene-age extension that affected the area [e.g., Lin *et al.*, 2003; Yang *et al.*, 2006; Rodriguez-Roa and Wiltschko, 2010]. Changes in thickness of the Miocene stratigraphy across, for example, the Chelungpu thrust indicate that reactivation of the Miocene-age faults is also taking place. This may, in part, account for changes in strike of the various thrusts in the Alishan area. Direct evidence for the reactivation of Eocene-aged extensional faults is difficult to infer from the surface geology alone. The *P* wave velocity model presented in Figures 7 and 8 may, however, provide key insights into this important question.

The *P* wave velocity model indicates that rocks with relatively high velocities are close to the surface beneath the Shuangtung thrust sheet as it widens southward through the Alishan area (Figures 8 and 9). We interpret a *V_p* of ≥ 5.2 km/s to be indicative of the presence of the Mesozoic clastic sedimentary basement rocks intersected in boreholes in western Taiwan [Chiu, 1975; Ho, 1988; Shaw, 1996]. While Chen and Yang [1996] and Tang and Zheng [2010] give these rocks a slightly lower *V_p* ($\leq \sim 5$ km/s), 5.2 km/s is in agreement with laboratory measurements of *V_p* of weakly metamorphosed polymictic clastic sediments (the bulk of the Cretaceous rocks found in boreholes in western Taiwan is arkosic sandstone, slate, and graywacke [Chiu, 1975]) at depths of 5 to 10 km [Christensen, 1989; Christensen and Mooney, 1995]. We suggest, then, that the 5.2 km/s isovelocity line (Figures 8 and 9) marks the approximate location of the contact between the Mesozoic basement and the overlying Eocene rocks. We stress, though, that 5.2 km/s provides only an estimate for the location of the top of the basement, as it is not possible to differentiate between it and the overlying Eocene rocks (of similar composition) on the basis of *V_p*. Nevertheless, if we accept that a *V_p* of 5.2 km/s is near the basement-synrift contact, then basement rocks are at a relatively shallow level in the crust beneath the Shuangtung thrust sheet (Figure 9b). This interpretation is different from that of Yang *et al.* [2007] and Tsai *et al.* [2012] who put large thicknesses of Miocene and younger rocks at depth in the Shuangtung thrust sheet, and more in agreement with Rodriguez-Roa and Wiltschko [2010] who put Paleogene and older rocks. As can be seen from Figures 7 and 8, the Miocene and younger rocks have a much lower *V_p* than do the rocks under the Shuangtung thrust sheet, suggesting that they are not present there [see also, Rau and Wu, 1995; Kim *et al.*, 2005, 2010; Wu *et al.*, 2007; Kuo-Chen *et al.*, 2012] (Figure 9).

Although we can interpret the uplift of basement rocks in the Shuangtung thrust sheet, this uplift does not account for the change in elevation of the Changhua and Chelungpu thrusts, and the stratigraphic contacts in their hanging walls (Figure 5). We therefore propose that there is reactivation and inversion of a NE striking extensional fault system (i.e., B and Yichu faults in Figure 1) that is resulting in the formation of the NE striking Choshui lateral structure (Figure 10). Inversion of this fault system is resulting in basement rocks (with velocities > 5.2) being uplifted, forming what is structurally termed a basement culmination. In this interpretation, the N-S fault (Figure 10) is a feature that is needed at depth to accommodate the uplift of these basement rocks. The basement culmination is developing in such a way that the Changhua-Chelungpu thrusts are being folded over the culmination wall developed in the hanging wall of the Choshui lateral structure (Figure 10). In this way, the basement culmination accounts for the north-south changes in elevation of structures (including branch lines) and stratigraphic contacts, as well as the change in strike and shallowing of the *V_p* isovelocity lines (which coincide with the change in strike of thrusts and with the southward change in elevation of stratigraphic contacts). The folding of the Changhua-Chelungpu thrusts above the basement culmination suggests that the sequence of thrusting initiated with the emplacement of the Shuangtung thrust followed by the Chelungpu thrust, then the Changhua thrust and later the development of the basement culmination. Today, all appear to be active at the same time. Based on the amount of uplift that can be determined from the change in elevation of stratigraphic contacts and the faults in our cross sections, we estimate that there is a minimum of 3 km of vertical displacement across this culmination wall (Figure 10a). It appears that there is displacement transferred westward along a deeper detachment level in the region to the south of the culmination wall. It is not possible to determine the horizontal displacement with the current data set.

6. Conclusions

In this paper we have mapped important changes in structure, stratigraphy, and seismic velocities across the Alishan area of Taiwan. Our new geological mapping, together with the geological cross sections, fault contour, stratigraphic cutoff, and branch line maps provide an estimate of a minimum amount of horizontal

shortening of about 15 km. Displacement directions along the Changhua, Chelungpu, and Shuangtung thrusts are, overall, roughly northwest directed. There is a several kilometer change in elevation of the location of the Changhua and Chelungpu thrusts, and stratigraphic contacts as they shallow southward. The P wave velocity model shows an increase in V_p from northwest to southeast across the area, with a V_p of ≥ 5.2 km/s coming to within 3 km of the surface within the Shuangtung thrust sheet. This higher V_p is interpreted to indicate the presence of basement rocks in the shallow subsurface throughout much of the southeastern part of the Alishan area.

The change in elevation of the thrust surfaces and stratigraphic contacts, taken together with the presence of higher V_p rocks (>5.2 km/s) in the shallow subsurface, suggests that there is a basement culmination forming beneath the Alishan area. This basement culmination can, in part, be explained by the uplift of rocks with these physical properties along the Shuangtung thrust. There are, however, changes in the Changhua and Chelungpu thrust surfaces and stratigraphic contacts in their hanging walls that suggest that there is uplift of rocks beneath the basal thrust that must account for a change of greater than 7 km in elevation of the base of the Cholan Formation. We interpret this to be the result of reactivation of preexisting northeast striking faults that affected the basement, folding the thrust system above it. We furthermore interpret it to be related to the B and Yichu group of faults found in the foreland and possibly their northeast extension into the Western Foothills. In this scenario, the changes in strike and elevation of fault surfaces and stratigraphic contacts that take place from north to south are associated with a feature that we call the Choshui lateral structure, which we interpret to reactivate the northeast striking basement faults (Figure 10).

Acknowledgments

This research was carried out with the aid of grants by CSIC—Proyectos Intramurales 2006 3 01 010 and MICINN: CGL2009-11843-BTE. The TAIGER local tomography data can be found at H. Kuo-Chen's personal web page at Taiwan's National Central University: http://www.cc.ncu.edu.tw/~kuochen/data/taiger_local.xyzv. All structural geological data presented in Figure 3 can be obtained from the lead author. The help and guidance provided by M.-M. Chen, H.-T. Chu, and C.-Y. Huang have been invaluable in our work in Taiwan. Reviews by J. Malaveille, T. Bryne, and P. Vannucchi helped clarify a number of points in the manuscript.

References

- Allmendinger, R. W., and P. A. Judge (2013), Stratigraphic uncertainty and errors in shortening from balanced sections in the North American Cordillera, *Geol. Soc. Am. Bull.*, *125*, 1569–1579.
- Brown, D., J. Alvarez-Marron, M. Schimmel, Y.-M. Wu, and G. Camanni (2012), The structure and kinematics of the central Taiwan mountain belt derived from geological and seismicity data, *Tectonics*, *31*, TC5013, doi:10.1029/2012TC003156.
- Butler, R. W. H., E. Tavarnelli, and M. Grasso (2006), Structural inheritance in mountain belts: An Alpine – Apennine perspective, *J. Struct. Geol.*, *28*, 1893–1908.
- Byrne, T., Y.-C. Chan, R.-J. Rau, C.-Y. Lu, Y.-H. Lee, and Y.-J. Wang (2011), The arc-continent collision in Taiwan, in *Arc-Continent Collision*, *Front. Earth Sci. Ser.*, edited by D. Brown and P. D. Ryan, pp. 213–245, Springer, Berlin Heidelberg.
- Camanni, G., D. Brown, J. Alvarez-Marron, Y.-M. Wu, and H.-A. Chen (2014), The Shuilikeng fault in central Taiwan mountain belt, *J. Geol. Soc.*, *171*, 117–130.
- Chen, A. T., and Y.-L. Yang (1996), Lack of compressional overprint on the extensional structure in offshore Tainan and the tectonic implications, *Terr. Atmos. Ocean*, *4*, 505–522.
- Chen, C.-H., et al. (2000), Geological Map of Taiwan. 1:500,000 scale, Central Geol. Sur., Taiwan.
- Chen, W.-S., K. D. Ridgway, C.-S. Horng, Y.-G. Chen, K.-S. Shea, and M.-G. Yeh (2001), Stratigraphic architecture, magnetostratigraphy, and incised-valley systems of the Pliocene-Pleistocene collisional marine foreland basin of Taiwan, *Geol. Soc. Am. Bull.*, *113*, 1249–1271.
- Chen, W.-S., et al. (2007), Late Holocene paleoearthquake activity in the middle part of the Longitudinal Valley Fault, eastern Taiwan, *Earth Planet. Sci. Lett.*, *264*, 420–437.
- Cheng, W.-B., H.-C. Huang, C. Wang, M.-S. Wu, and T.-H. Hsuan (2003), Velocity structure, seismicity, and fault structure in the Peikang High area of western Taiwan, *Terr. Atmos. Ocean*, *14*, 63–83.
- Ching, K.-E., R.-J. Rau, K. M. Johnson, J.-C. Lee, and J.-C. Hu (2011), Present-day kinematics of active mountain building in Taiwan from GPS observations during 1995–2005, *J. Geophys. Res.*, *116*, B09405, doi:10.1029/2010JB008058.
- Chiu, H.-T. (1975), Miocene stratigraphy and its relation to the Palaeogene rocks in west-central Taiwan, *Pet. Geol. Taiwan*, *12*, 51–80.
- Christensen, N. I. (1989), Seismic velocities, in *CRC Practical Handbook of Physical Properties of Rocks and Minerals*, edited by R. S. Carmichael, pp. 429–546, CRC Press, Boca Raton.
- Christensen, N. I., and W. D. Mooney (1995), Seismic velocity structure and composition of the continental crust: A global view, *J. Geophys. Res.*, *100*, 9761–9788, doi:10.1029/95JB00259.
- Covey, M. (1984), Lithofacies analysis and basin reconstruction, Plio-Pleistocene Western Taiwan foredeep, *Pet. Geol. Taiwan*, *20*, 53–83.
- Covey, M. (1986), The evolution of foreland basins to steady state: Evidence from the western Taiwan foreland basin, in *Foreland Basins*, *Int. Assoc. Sedimentol. Spec. Publ.*, vol. 8, edited by P. A. Allen and P. Homewood, pp. 77–90, Blackwell, Oxford, U. K.
- Chinese Petroleum Company (CPC) (1986), Geologic Map No. 5, Chiayi. Scale: 1:100000. Taiwan Petroleum, Exploration Division, Chinese Petroleum Company, Taipei, Taiwan.
- Dahlstrom, C. D. A. (1969), Balanced cross sections, *Can. J. Earth Sci.*, *6*, 743–757.
- Ding, W.-W., J.-B. Li, M.-B. Li, X.-L. Qiu, Y.-X. Fang, and Y. Tang (2008), A Cenozoic tectono-sedimentary model of the Tainan Basin, the South China Sea: Evidence from multi-channel seismic profile, *J. Zhejiang Univ. Sci. A*, *9*, 702–713.
- Eakin, D. H., K. D. McIntosh, H. J. A. van Avendonk, L. Lavier, R. Lester, C.-S. Liu, and C.-S. Lee (2014), Crustal-scale seismic profiles across the Manila subduction zone: The transition from intraoceanic subduction to incipient collision, *J. Geophys. Res. Solid Earth*, *119*, 1–17, doi:10.1002/2013JB010395.
- Faulds, J. E., and R. J. Varga (1998), The role of accommodation zones and transfer zones in the regional segmentation of extended terranes, in *Accommodation Zones and Transfer Zones; the Regional Segmentation of the Basin and Range Province*, *Geol. Soc. Am. Spec. Pap.*, *323*, 1–45, doi:10.1130/0-8137-2323-X.1.

- Flöttmann, T., and P. James (1997), Influence of basin architecture on the style of inversion and fold-thrust belt tectonics – The southern Adelaide Fold-Thrust Belt, South Australia, *J. Struct. Geol.*, *19*, 1093–1110.
- Hall, R. (1996), Reconstructing Cenozoic SE Asia, in *Tectonic Evolution of Southeast Asia*, edited by R. Hall and D. Blundell, *Geol. Soc. London Spec. Publ.*, *106*, 153–184.
- Hall, R. (2001), Cenozoic reconstructions of SE Asia and the SW Pacific: Changing patterns of land and sea, in *Faunal and Floral Migrations and Evolution in SE Asia-Australasia*, edited by I. Metcalfe, pp. 35–56, Swets and Zeitlinger, Lisse.
- Ho, C.-S. (1988), *An Introduction to the Geology of Taiwan: Explanatory Text of the Geological Map of Taiwan*, Central Geol. Sur, Taipei, Taiwan.
- Hong, E. (1997), Evolution of Pliocene to Pleistocene sedimentary environments in an arc-continent collision zone: Evidence from analyses of lithofacies and ichnofacies in the southwestern foothills of Taiwan, *J. Asian Earth Sci.*, *15*, 381–392.
- Hossack, J. R. (1979), The use of balanced cross-sections in the calculation of orogenic contraction: A review, *J. Geol. Soc. London*, *136*, 705–711.
- Hsu, S.-K., Y.-C. Yeh, W.-B. Doo, and C.-H. Tsai (2004), New bathymetry and magnetic lineations identifications in the northernmost South China Sea and their tectonic implications, *Mar. Geophys. Res.*, *25*, 29–44.
- Huang, C.-S., K.-S. Shea, and M.-M. Chen (2000), Geological map of Taiwan: Sheet 32, Puli, Central Geol. Sur. Taiwan.
- Huang, C.-Y., W.-Y. Wu, C.-P. Chang, S. Tsao, P.-B. Yuan, C.-W. Lin, and K.-Y. Xia (1997), Tectonic evolution of accretionary prism in the arc-continent collision terrane of Taiwan, *Tectonophysics*, *281*, 31–51.
- Huang, C.-Y., K. Xia, P. B. Yuan, and P.-G. Chen (2001), Structural evolution from Paleogene extension to Latest Miocene-Recent arc-continent collision offshore Taiwan: Comparison with on land geology, *J. Asian Earth Sci.*, *19*, 619–639.
- Jahn, B.-M., W.-R. Chi, and T.-F. Yui (1992), A Late Permian formation of Taiwan (marbles from Chia-Li well No.1): Pb-Pb isochron and Sr isotopic evidence, and its regional geological significance, *J. Geol. Soc. China*, *35*, 193–218.
- Judge, P. A., and R. W. Allmendinger (2011), Assessing uncertainties in balanced cross sections, *J. Struct. Geol.*, *33*, 458–467.
- Kim, K.-H., J.-M. Chiu, J. Pujol, K.-C. Chen, B.-S. Huang, Y.-H. Yeh, and P. Shen (2005), Three-dimensional VP and VS structural models associated with the active subduction and collision tectonics in the Taiwan region, *Geophys. J. Int.*, *162*, 204–220.
- Kim, K.-H., K.-C. Chen, J.-H. Wang, and J.-M. Chiu (2010), Seismogenic structures of the 1999 Mw 7.6 Chi-Chi, Taiwan, earthquake and its aftershocks, *Tectonophysics*, *489*, 119–127.
- Kuo-Chen, H., F. T. Wu, and S. W. Roecker (2012), Three-dimensional P velocity structures of the lithosphere beneath Taiwan from the analysis of TAIGER and related seismic data sets, *J. Geophys. Res.*, *117*, B06306, doi:10.1029/2011JB009108.
- Lee, T.-Y., and L. A. Lawver (1994), Cenozoic plate reconstruction of the South China Sea region, *Tectonophysics*, *235*, 149–180.
- Li, C.-F., Z. Zhou, J. Li, H. Hao, and J. Geng (2007), Structures of the northeasternmost South China Sea continental margin and ocean basin: Geophysical constraints and tectonic implications, *Mar. Geophys. Res.*, *28*, 59–79.
- Lin, A. T.-S., and A. Watts (2002), Origin of the west Taiwan basin by orogenic loading and flexure of a rifted continental margin, *J. Geophys. Res.*, *107*(B9), 2185, doi:10.1029/2001JB000669.
- Lin, A., A. Watts, and P. Hesselbo (2003), Cenozoic stratigraphy and subsidence history of the South China Sea margin in the Taiwan region, *Basin Res.*, *15*, 453–478, doi:10.1046/j.1365-2117.2003.00215.x.
- Lin, A. T., C.-S. Liu, C.-C. Lin, P. Schnurle, G.-Y. Chen, W.-Z. Liao, L. S. Teng, H.-J. Chuang, and M.-S. Wu (2008), Tectonic features associated with the overriding of an accretionary wedge on top of a rifted continental margin: An example from Taiwan, *Mar. Geol.*, *255*, 186–203.
- Liu, H.-C., J.-F. Lee, and C.-C. Chi (2004), Geological map of Taiwan: Sheet 38, Yulin, Central Geol. Sur. Taiwan.
- Malavielle, J., S. E. Lallemand, S. Dominguez, A. Deschamps, C.-Y. Lu, C. A. Liu, P. Schnürle, and ACT Scientific Crew (2002), Arc-continent collision in Taiwan: New marine observations and tectonic evolution, in *Geology and Geophysics of an Arc-Continent Collision, Taiwan*, edited by T. B. Byrne and C.-S. Liu, *Geol. Soc. Am. Spec. Pap.*, *358*, 187–211.
- Manatschal, G. (2004), New models for the evolution of magma-poor rifted margins based on a review of data and concepts from West Iberia and the Alps, *Int. J. Earth Sci.*, *93*, 432–466.
- Mohn, G., G. Manatschal, M. Beltrando, E. Masini, and N. Kusnir (2012), Necking of the continental crust in magma-poor rifted margins: Evidence from fossil Alpine Tethys margins, *Tectonics*, *31*, doi:10.1029/2011TC002961.
- Mouthereau, F., and O. Lacombe (2006), Inversion of the Paleogene Chinese continental margin and thick-skinned deformation in the Western Foreland of Taiwan, *J. Struct. Geol.*, *28*, 1977–1993.
- Mouthereau, F., O. Lacombe, B. Deffontaines, J. Angelier, and S. Brusset (2001), Deformation history of the southwestern Taiwan foreland thrust belt: Insights from tectono-sedimentary analyses and balanced cross-sections, *Tectonophysics*, *333*, 293–322.
- Mouthereau, F., B. Deffontaines, O. Lacombe, and J. Angelier (2002), Variations along the strike of the Taiwan thrust belt: Basement control on structural style, wedge geometry, and kinematics, in *Geology and Geophysics of an Arc-Continent Collision, Taiwan*, edited by T. B. Byrne and C.-S. Liu, *Geol. Soc. Am. Spec. Pap.*, *358*, 31–54.
- Nagel, S., S. Castellort, A. Wetzel, S. D. Willett, F. Mouthereau, and A. T. Lin (2013), Sedimentology and foreland basin paleogeography during Taiwan arc continent collision, *J. Asian Earth Sci.*, *62*, 180–204.
- Rau, R.-J., and F. T. Wu (1995), Tomographic imaging of lithospheric structures under Taiwan, *Earth Planet. Sci. Lett.*, *133*, 517–532.
- Reston, T. J. (2009), The structure, evolution and symmetry of the magma poor rifted margins of the North and Central Atlantic: A synthesis, *Tectonophysics*, *468*, 6–27.
- Reston, T. J., and G. Manatschal (2011), Rifted margins: Building blocks of later collision, in *Arc-Continent Collision, Front. Earth Sci. Ser.*, edited by D. Brown and P. D. Ryan, pp. 3–21, Springer, Berlin Heidelberg.
- Rodriguez-Roa, F. A., and D. V. Wiltschko (2010), Thrust belt architecture of the central and southern Western Foothills of Taiwan, in *Hydrocarbons in Contractual Belts*, edited by G. P. Goffey et al., *Geol. Soc. London Spec. Publ.*, *348*, 137–168.
- Shaw, C.-L. (1996), Stratigraphic correlation and isopach maps of the Western Taiwan Basin, *TAO*, *7*, 333–360.
- Shea, K.-S., H.-C. Chang, T.-Y. Huang, H.-C. Ho, W.-H. Lin, C.-W. Lin, and H.-W. Chen (2003), *Geological Column in Taiwan*, Central Geological Survey of Taiwan, Taiwan.
- Shyu, J. B. H., K. Sieh, Y.-G. Chen, R.-Y. Chuang, Y. Wang, and L.-H. Chung (2008), Geomorphology of the southernmost Longitudinal Vally Fault: Implications for evolution of the active suture of eastern Taiwan, *Tectonics*, *27*, TC1019, doi:10.1029/2006TC002060.
- Sibuet, J. C., and S.-K. Hsu (1997), Geodynamic of the Taiwan arc-continent collision, *Tectonophysics*, *274*, 221–252.
- Sibuet, J. C., and S.-K. Hsu (2004), How was Taiwan created?, *Tectonophysics*, *379*, 159–181.
- Smith, N. T. (1999), Variscan inversion within the Cheshire Basin, England: Carboniferous evolution north of the Variscan Front, *Tectonophysics*, *309*, 211–225.
- Suppe, J. (1980), A retrodeformable cross section of northern Taiwan, *Proc. Geol. Soc. China*, *23*, 46–55.
- Suppe, J. (1984), Kinematics of arc-continent collision, flipping of subduction, and back-arc spreading near Taiwan, *Mem. Geol. Soc. China*, *6*, 21–33.

- Tang, Q., and C. Zheng (2010), Seismic velocity structure and improved seismic image of the Southern Depression of the Tainan Basin from pre-stack depth migration, *Terr. Atmos. Ocean. Sci.*, *21*, 807–816.
- Teng, L. S. (1987), Stratigraphic records of the Late Cenozoic Penglai Orogeny of Taiwan, *Acta Geol. Taiwanica*, *25*, 205–224.
- Teng, L.-S. (1990), Geotectonic evolution of the late Cenozoic arc-continent collision in Taiwan, *Tectonophysics*, *183*, 57–76.
- Teng, L.-S. (1992), Geotectonic evolution of Tertiary continental margin basins of Taiwan, *Pet. Geol. Taiwan*, *27*, 1–19.
- Teng, L.-S., and A.-T. Lin (2004), Cenozoic tectonics of the China continental margin; Insights from Taiwan, in *Aspects of the Tectonic Evolution of China*, edited by J. Malpas et al., *Geol. Soc. London Spec. Publ.*, *226*, 313–332.
- Tensi, J., F. Mouthereau, and O. Lacombe (2006), Lithospheric bulge in the West Tainan Basin, *Basin Res.*, *18*, 277–299.
- Tsai, M.-C., S.-B. Yu, Y.-J. Hsu, H.-Y. Chen, and H.-W. Chen (2012), Interseismic crustal deformation of frontal thrust fault system in the Chiayi-Tainan area, Taiwan, *Tectonophysics*, *554-557*, 169–184.
- Wang, C.-Y., C.-L. Li, F.-C. Su, M.-T. Leu, M.-S. Wu, S.-H. Lai, and C.-C. Chern (2002), Structural mapping of the 1999 Chi-Chi earthquake fault, Taiwan, by seismic reflection methods, *Terr. Atmos. Ocean. Sci.*, *13*, 211–226.
- Wu, Y.-M., C.-H. Chang, L. Zhao, J. B. H. Shyu, Y.-G. Chen, K. Sieh, and J. P. Avouac (2007), Seismic tomography of Taiwan: Improved constraints from a dense network of strong motion stations, *J. Geophys. Res.*, *112*, B08312, doi:10.1029/2007JB004983.
- Wu, Y.-M., Y.-J. Hsu, C.-H. Chang, L.-S. Teng, and M. Nakamura (2010), Temporal and spatial variation of stress field in Taiwan from 1991 to 2007: Insights from comprehensive first motion focal mechanism catalog, *Earth Planet. Sci. Lett.*, *298*, 306–316, doi:10.1016/j.epsl.2010.07.047.
- Yagupsky, D. L., E. O. Cristallini, J. Fantín, G. Z. Valcarce, G. Bottesi, and R. Varadé (2008), Oblique half-graben inversion of the Mesozoic Neuquén Rift in the Malargüe Fold and Thrust Belt, Mendoza, Argentina: New insights from analogue models, *J. Struct. Geol.*, *30*, 839–853.
- Yang, K.-M., H.-H. Ting, and J. Yuan (1991), Structural styles and tectonic modes of Neogene extensional tectonics in southwestern Taiwan: Implication for hydrocarbon exploration, *Pet. Geol. Taiwan*, *26*, 1–31.
- Yang, K.-M., S.-T. Huang, J.-C. Wu, H.-H. Ting, and W.-W. Mei (2006), Review and insights on foreland tectonics in western Taiwan, *Int. Geol. Rev.*, *48*, 910–941.
- Yang, K.-M., S.-T. Huang, J.-C. Wu, H.-H. Ting, W.-W. Mei, M. Lee, H.-H. Hsu, and C.-J. Lee (2007), 3D geometry of the Chelungpu thrust system in Central Taiwan: Its implications for active tectonics, *Terr. Atmos. Ocean. Sci.*, *18*, 143–181.
- Yeh, Y.-C., and S.-K. Hsu (2004), Crustal structure of the northernmost South China Sea: Seismic reflection and gravity modeling, *Mar. Geophys. Res.*, *25*, 45–61.
- Yu, H.-S. (2004), Nature and distribution of the deformation front in the Luzon arc-Chinese continental margin collision zone at Taiwan, *Mar. Geophys. Res.*, *25*, 109–122.
- Yu, H.-S., and Y.-W. Chou (2001), Characteristics and development of the flexural forebulge and basal unconformity of western Taiwan foreland basin, *Tectonophysics*, *333*, 277–291.
- Yu, H.-S., and S.-J. Lin (1991), A preliminary study of seismic stratigraphy of the Late Cenozoic sequences in the Tainan Basin off southwestern Taiwan, *Terr. Atmos. Ocean. Sci.*, *2*, 75–94.
- Yu, S.-B., and L. C. Kuo (2001), Present day crustal motion along the Longitudinal Valley Fault, eastern Taiwan, *Tectonophysics*, *333*, 199–217.
- Yu, S.-B., H. Y. Chen, and L. C. Kuo (1997), Velocity field of GPS stations in the Taiwan area, *Tectonophysics*, *274*, 41–60.
- Yue, L.-F., J. Suppe, and J.-H. Hung (2005), Structural geology of a classic thrust belt earthquake: the 1999 Chi-Chi earthquake Taiwan (Mw = 7.6), *J. Struct. Geol.*, *27*, 2058–2083.
- Zanchi, A., F. Berra, M. Mattei, M. R. Ghassemi, and J. Sabouri (2006), Inversion tectonics in the central Alboraz, Iran, *J. Struct. Geol.*, *28*, 2023–2037.